

# Quasar candidate multicolor selection technique: a different approach

E. Hatziminaoglou, G. Mathez, and R. Pelló

Observatoire Midi-Pyrénées, Laboratoire d'Astrophysique, UMR 5572, 14 Avenue E. Belin, 31400 Toulouse, France

Received 1 February 2000 / Accepted 28 April 2000

**Abstract.** We present a quasar candidate identification technique based on multicolor photometry. The traditional multi-dimensional method ( $2 \times N$  dimensions, where  $N$  is the number of the color-color diagrams) is reduced to a one-dimensional technique, which consists in a standard fitting procedure, where the observed spectral energy distributions are compared to quasar simulated spectra and stellar templates. This new multicolor approach is firstly applied to simulated catalogues and its *efficiency* is examined in various redshift ranges, as a function of the filter combination and the available observing time for spectroscopy. We conclude that this method is better suited than the usual multicolor selection techniques to quasar identification, especially for high-redshift quasars. The application of the method to real quasar samples found in the literature results in an *efficiency* comparable to the one obtained from the use of color-color diagrams. The major advantage of the new method is the estimation of the *photometric* redshift of quasar candidates, enabling, in almost all cases, spectroscopy to be targeted to best suited wavelength ranges.

**Key words:** galaxies: photometry – galaxies: quasars: general – cosmology: miscellaneous

## 1. Introduction

Nowadays, very high redshift galaxies and quasars are being found. However, quasars still offer the opportunity of a (relatively) easy construction of high- $z$  samples, due to their high luminosity, quasi-stellar shape (allowing accurate photometry), and to their emission lines (allowing spectroscopical identification). Therefore, many large optical quasar surveys are in progress or in project. Even if high energy emission is quite a common quasar property, X-ray samples still need the detection of emission lines in the optical domain for the purposes of redshift determination. To improve the efficiency of all quasar studies, one has to increase both the size and the upper redshift limit of the sample, and to achieve a maximum completeness over a redshift range as large as possible.

These surveys are essentially based on the photometric pre-selection of quasar candidates, in order to optimize the effi-

ciency of telescope time. Preselection makes the completeness questionable both at low and at high redshift (see discussion in e.g. Miller & Mitchell, 1998). Even multiple color-color diagrams (e.g. Hall et al., 1996b) still reveal a bias in the range  $2.2 \leq z \leq 3$ , exactly where a reversing of evolution is thought to occur, making completeness specially important. At low redshift, it has been shown that the usual morphologic prerequisite for *quasi-stellar* candidates results in a noticeable deficiency (Wolf et al., 1999). This trend may increase the apparent evolution of quasars.

The present paper describes a joint method both for distinguishing between quasars and stars/galaxies by their photometry *and* for obtaining an estimate of the photometric redshift of the quasar candidates as well. In Sect. 2 we present the current state of the art in the optical search for quasars. Sect. 3 gives a brief description of our method, which has been first validated with simulations, as shown in Sect. 4, before being applied to real samples (Sect. 5). The last section of this paper (Sect. 6) contains a summary of our conclusions and a brief discussion.

## 2. State of the art in the optical search for quasars

One of the most common problems in optical surveys is the selection criteria one has to apply in order to distinguish between stars and quasars, since both categories of objects have (in most cases) a point-like morphology. Quasars are spatially resolved only at low redshifts and only when high quality imaging data are available. Selection of QSO candidates among stellar objects from photometric data is becoming a standard method. The UVX technique (UV excess) separates stars from quasars with a redshift  $z \leq 2.2$ . This technique is still currently being used, e.g. in the *Chile-UK quasar survey* (CUQS), and the *AAT 2dF QSO Survey*.

To avoid both the redshift limitation ( $z < 2.2$ ) and the bias towards blue objects, other equivalent techniques are also being applied (for example BRX), with quite a high efficiency in other redshift ranges. Many Multicolor Surveys use an increased number of filters, especially towards the red, with special care paid to high- $z$  quasars: examples are found in Boyle et al. (1991), Kenefick et al. (1997), Osmer et al. (1998) and the references therein, Jarvis & Mac Alpine (1998) and the *DPOSS* (Digital POSS II). In all these cases, the efficiency never exceeds 35%

---

Send offprint requests to: E. Hatziminaoglou (eva@ast.obs-mip.fr)

( $\simeq 3$  candidates selected per one real quasar), depending on magnitude and redshift.

For all the selection methods described above, the working space is the  $N \times 2D$ -manifold of  $N$  color-color planes. The locus of quasars at different redshifts in each of these planes is compared to the locus expected for Main Sequence stars. For quasars, the allowed multi-color space is defined through simulated template spectra, set to different redshifts. Basically all the selection procedures use the positions of candidates in the multi-color space either to compare with the expected locus for quasars or to compute the distance to the Main Sequence (Newberg & Yanny, 1997; Sloan Digital Sky Survey - Fan, 1999; Krisciunas et al., 1998). Quasar candidates are among the objects at the largest distances with respect to this Main Sequence “Snake”. However the selection of candidates with quasar spectra is basically a 1D problem: the fitting between the observed spectral energy distribution (SED) and the equivalent one obtained from templates (quasars/stars), all of them computed within the same photometric system. Two quasar surveys make use of such a fit to select candidates and to estimate their photometric redshifts. The Calar Alto Deep Imaging Survey (*CADIS*) uses specialized filters and a multicolor classification algorithm to distinguish between stars, galaxies and quasars, and the identification of high- $z$  quasars in particular is based on the photometric redshift method (Wolf et al., 1999). The *Large Zenith Telescope*, a 6-meter liquid-mirror telescope, will provide photometric redshifts for more than 1 million of galaxies, thanks to a series of 40 medium-band filters specially designed, and will be able to select quasar candidates quite efficiently. For the purposes of this paper, even a reduced set of broad band photometric data on a given object shall be considered as a very low resolution spectrum ( $R \sim 1!$ ), which could be fitted by synthetic templates according to the standard methods commonly used on photometric redshift estimates. Assumptions on the morphology of the objects could be avoided in principle, in such a way that both point-like and spatially resolved sources could be examined through the same pipeline. Furthermore, it is interesting to have a prior idea on the redshift range of each candidate, in order to perform the spectroscopic follow up in the suitable wavelength range (visible or IR).

The software described in the present paper has been developed for the needs of preparing the quasars/AGN sample to be assembled in the future VIRMOS survey. It can however be applied to all multicolor catalogues. The forthcoming VIRMOS spectroscopic galaxy survey will consist in 2 surveys: a deep one and a shallow one. The VIRMOS-SHALLOW spectroscopic sample (statistically 1/4 to 1/3 complete to  $I \leq 22.5$ , no other preselection) will ensure random completeness, without any color or morphology preselection. The VIRMOS-DEEP survey (complete for all objects with  $22.5 < I \leq 24$ ) will provide the opportunity of assembling a quasar sample avoiding the drawbacks of any preselection, therefore basically free of the usual biases (colors, redshift etc). So far, very few such samples are available: three examples come from the CFRS ( $I=22.5$ , Schade et al., 1995), the Faint Galaxy Redshift Survey ( $B=24$ , Glazebrook et al., 1995) and more recently Cohen et al. (1999)

to  $R=24$  in the HDF, involving, however, very few quasars. We are examining various possibilities of assembling a third quasar sample in the limits of the VIRMOS-SHALLOW survey, trying to get as much as possible of the spectra of the several thousands of quasars present in this field by selecting photometric candidates. Comparing the three VIRMOS samples should provide a unique opportunity of examining the biases introduced by a photometric and/or morphological preselection on the quasar samples.

### 3. Description of the method

Our method used here is closely based on *hyperz*, a public photometric redshift code presently under development at the Observatoire Midi-Pyrénées. Details on *hyperz* will be given in a forthcoming paper (Bolzonella et al., 2000; see also Miralles & Pelló, 1998; Pelló et al., 1999). It is basically a standard SED fitting procedure: the observed photometric SED of a given object, obtained through  $n$  filters, is compared to the SED computed for a set of template spectra. The aim is to find the best fit between the observed and the model photometry through a standard  $\chi^2$  minimization procedure:

$$\chi^2 = \sum_{i=1}^n \frac{(F_{obs}^i - F_{mod}^i(z))^2}{\sigma_i^2}$$

where  $F_{obs}^i$  and  $F_{mod}^i$  are respectively the observed and the template fluxes in the  $i$  band, and  $\sigma_i$  is the error on the observed flux in this band. Fluxes are normalized to an arbitrary reference filter. This is a quite general method. The photometric redshift is the redshift  $z$  corresponding to the minimum  $\chi^2$  value. As expected, the accuracy on the photometric redshift determination depends strongly on the set of filters used (number and wavelength coverage); this is illustrated in the next paragraph.

In order to apply this method to quasars, the template set is made by series of simulated quasar spectra. These spectra have been constructed by varying the slope of the power-law spectra (spectral index) in the optical (between 0.0 and 1.0, in 3 steps) while keeping the ultraviolet index,  $a_{UV}$ , constant at 1.76 (a value compatible with Wang et al., 1998). Emission lines are included ( $Ly_{\alpha}$ ,  $Ly_{\beta}$ , CIII, CIV, MgII, SiIV,  $H_{\alpha}$ ,  $H_{\beta}$  and  $H_{\gamma}$ ) with gaussian profiles and typical intensities (e.g. Peterson, 1997), as well as the small blue bump, centered at 3000 Å. The redshift value is set between 0 and 7. Totally, there are 213 quasar spectra, with 71 redshift steps ( $dz = 0.1$ ), with 3 simulated spectra on each step, obtained by varying the optical spectral index. The  $Ly_{\alpha}$  forest has been modeled according to Madau (1995), while no reddening has been included. We also included the stellar library of Pickles (1998), which contains 108 spectra of stellar types ranging from O to M, including dwarfs and giant stars. Additionally, we included 22 white dwarf and carbon stars spectra, which are known to contaminate the quasar candidates catalogues.

When applying the method to a given sample, the discrimination between stars and quasars is performed in two steps. A first distinction between stars and quasars is made by identifying as star (quasars) the objects that show a better fit to one of

the stellar (quasar) spectra. A further selection on the remaining sample can be made, based on the value of the reduced  $\chi^2$ , with stars identified as objects excluded as quasars at the 95% or 99% confidence levels. In the present paper, the terms “ $\chi^2$  selection” or “no  $\chi^2$  selection” will apply for such a distinction. When an object is identified as quasar candidate, a photometric redshift estimation is automatically provided. The number of degrees of freedom,  $\nu$ , is equal to the number of filters minus 2: we lose one degree by normalizing the flux to a reference filter and one degree because of the “best fit” procedure. In this way, the separation between stars and quasars is reduced to a one-dimensional fit between the data (the observed SED) and the spectral templates.

As expected, and as confirmed by the simulations, the quality of the quasar/star discrimination depends on the filter combination, as it happens for the photometric redshift estimate in the case of galaxies. Not only the number of filters is important, but also the wavelength range covered. Another important point is the width of the filters which must be suited to the width of quasar spectral features. A realistic determination of the photometric errors is the key to a successful issue for this method.

#### 4. Simulations

The first test of this method has been done on mixed (quasars + stars) simulated catalogues. In this paragraph we intend to show the importance of the set of filters used for optimizing the results. First, let us define an arbitrary and useful quantity which is aimed to quantify the efficiency of this procedure. Let  $N_c$  be the number of quasar candidates resulting from the identification technique,  $N_f$  the number of actual quasars found as candidates (real quasars effectively selected), and  $N_e$  the number of expected quasars. In principle,  $N_e$  is a quantity which can be estimated from previous surveys. We define the “*efficiency*” of the method as follows:

$$\text{efficiency} = \text{completeness} \times \text{confirmation rate},$$

where  $\text{completeness} = N_f/N_e$  and  $\text{confirmation rate} = N_f/N_c$ . Obviously, both the *completeness* and the *confirmation rate* take values in the interval [0,1] and so does the *efficiency*.

The number of stars in our simulated catalogues was given by the Galaxy model of Robin et al., 1995 (R95). The star counts correspond to the six Deep Multicolor Survey (hereafter DMS) fields, since we primarily tested our results with the results of this survey. The fields with their surface (in square arc minutes) and the estimated star numbers are given in Table 1. Quasar numbers were based on previous surveys (Hartwick & Schade, 1990, hereafter HS90). Catalogues contain  $\sim 100$  quasars and  $\sim 3000$  stars, with a magnitude limit of  $m_b = 22.2$  and photometric errors scaling with magnitude, with typical values of the order of 0.1 magnitudes. Quasars are uniformly distributed in redshift, in order to obtain reasonable statistical results at all redshifts.

Photometry in broad-band filters has been simulated, covering the wavelength range between  $\sim 3000 \text{ \AA}$  and  $\sim 20000 \text{ \AA}$ : U, B, V, R, I, H, and K. Broad-band filters have been used for practical reasons, in particular because they directly apply to

**Table 1.** The six DMS fields, galactic coordinates, surfaces and estimated star numbers.

$l$	$b$	surface (sq')	stars
250	47	286	219
129	-63	516	263
77	35	552	826
337	57	561	581
52	-39	537	922
68	-51	537	505

the VIRMOS survey, which will make use of wide-band filters only, although narrow-band filters would give better results (Peri et al. 1997). 40 different filter combinations have been tested in the aim of selecting quasar candidates. Fig. 1a and b illustrate the *completeness* (solid line), *confirmation rate* (dashed line) and *efficiency* (dash-dotted line) for these 40 combinations, without any  $\chi^2$  selection and with selection at 99% confidence level, respectively. The filter combinations in Fig. 1a have been classified by increasing *completeness*. The same order has been used in Fig. 1b, to demonstrate the effect of a  $\chi^2$  selection on the *completeness* and the other parameters. Table 2 shows the filter combination which corresponds to the abscissa values.

A closer look at Fig. 1 and Table 2 reveals that the filter combination is, most of the time, more important than the number of filters. In general, filters like U or the infrared filters H and/or K are very useful: they add much photometric information constraining the number of candidates. Neighboring filters like B, V, R, when used all together, decrease the *efficiency* because, as mentioned above, they increase the number of the degrees of freedom without adding any essential information. A comparison of the two figures reveals several trends. The *completeness* is almost not influenced by a  $\chi^2$  selection in the case of 3-filter combinations (such as UBV, BRI, BVR, BVI, or UBR). It is, however, strongly influenced by a  $\chi^2$  selection when the filter U is present, in sets of 4 or more filters. Note that this quantity decreases significantly, when a  $\chi^2$  selection is imposed, for filter combinations with index higher than 26, which are all sets containing the U-filter. Furthermore, the *confirmation rate* is generally increasing with increasing number of filters. The decision whether to make a  $\chi^2$  selection or not depends on the available time for spectroscopy and the scientific objectives of the project.

For this purpose, we made an approximative estimation of the time needed for making the spectroscopy in order to cover an area of 1 square degree,  $T_{sp}$ , for the same 40 filter combinations, given a detector area,  $S$ , a magnitude limit,  $m_b$ , a quasar candidate density,  $n_q = N_{cand}/S$  (depending on this limit as well as on the filter combination), a number of slits,  $G$  and an exposure time,  $dT_{sp}$ , with and without any  $\chi^2$  selection. We calculate  $T_{sp}$  as:

$$T_{sp} = \left\{ 1 + \text{int} \left( \frac{N_{cand}}{G} \right) \right\} \times \frac{dT_{sp}}{S}$$

Fig. 2 illustrates  $T_{sp}$  (in hours) for  $m_b = 22.2$ ,  $S = 0.06$  square degrees,  $G = 10$  and  $dT_{sp} = 3$  hours, without any preselection

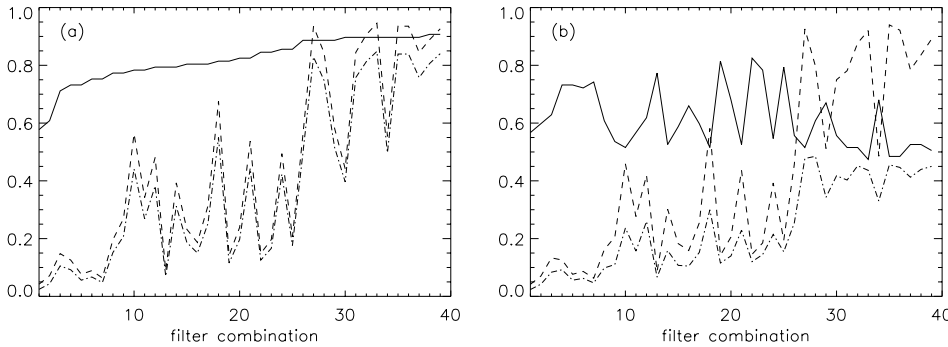


**Fig. 1a and b.** *completeness* (solid line), *confirmation rate* (dashed line) and *efficiency* (dash-dotted line) for 40 filter combinations, **a** without any  $\chi^2$  selection and **b** with selection at a 99% confidence level.

**Table 2.** Filter combinations used in Figs. 1a and 1b, classified by increasing *completeness* in the case of no  $\chi^2$  selection.

No	filters	No	filters	No	filters	No	filters	No	filters
1	VRI	2	VRH	3	BRH	4	UBV	5	BRI
6	BVRI	7	BVR	8	VIK	9	BVRIH	10	BRIHK
11	VRIHK	12	BRHK	13	BVI	14	BRIK	15	VRIK
16	BVK	17	RIHK	18	BVRIHK	19	UBR	20	UBH
21	BVRIK	22	UBVR	23	UBRI	24	BVIK	25	UBVRI
26	UBVRIK	27	UBVRIH	28	UBRHK	29	UBHK	30	UBVRK
31	UVIK	32	UVRIK	33	UBVRIHK	34	UVK	35	UBRIHK
36	UBVIHK	37	UBVRHK	38	UVIHK	39	UVRIHK	40	UBRIK

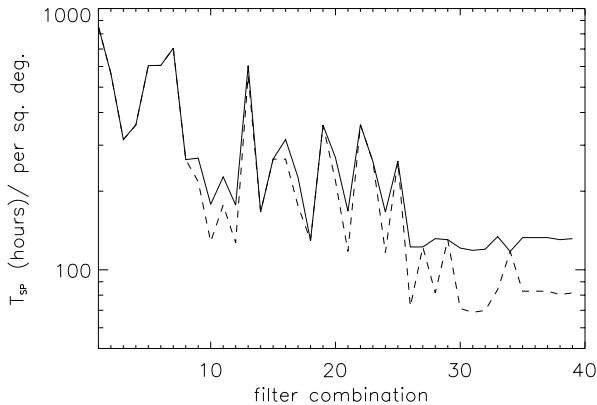


**Fig. 2.** Spectroscopy time (plotted on a logarithmic axis) per square degree versus filter combination, without any  $\chi^2$  preselection (solid line) and with a 99% confidence level selection (dashed line).

(solid line) and with a  $\chi^2$  selection (dashed line). Note that the y-axis is logarithmic. As expected, there is an anticorrelation between  $T_{sp}$  and the *confirmation rate*, as it appears from the comparison of Figs. 1 and 2. The highest the *confirmation rate*, the less time is required.

#### 4.1. Determination of the photometric redshifts

The problem of the quasar photometric redshift (hereafter  $z_{phot}$ ) estimation is at least as complex as the one for galaxies. Quasar spectral features (mainly emission lines) are rather narrow and the overall shape of the ultra-violet and optical continuum is a single power law, while the filters commonly used for photometry are wide-band filters, not very suitable for the quasar characteristics. All the above are in the origin of the dispersed

values of the estimated quasar  $z_{phot}$ , when compared to the spectroscopic ones, especially for quasars with redshifts lower than  $\sim 2$ . The filter combination is very important for the accurate determination of the  $z_{phot}$ . Fig. 3 shows the photometric redshift versus the model redshift, for a catalogue of 1540 simulated quasars, uniformly distributed over the redshift range [0,6], and for 4 different filter combinations. From top to bottom and left to right the following filter combinations are illustrated: BVRI (a), BVIK (b), UBVR (c), UBVRIK (d).

The use of the filter set BVRI is clearly a bad choice: these four filters cover a relatively short wavelength range and their effective wavelengths lie close to each other. The  $z_{phot}$  in this case is poorly determined for  $z \leq 3$ , while there is also a large dispersion at  $z \geq 5$ . If we replace the R-filter by the K-filter (Fig. 3b), the dispersion becomes more important at redshifts higher than 4, since this is the redshift at which  $Ly_{\alpha}$  should enter the R-band, but it decreases the dispersion at redshifts lower than 3, due to the very large wavelength range covered. Adding the filter U to the BVRI combination decreases the dispersion at both high and low redshifts (Fig. 3c), but one can still feel the absence of an infrared filter, whose importance is seen in Fig. 3d. The periodic accumulations of points at different redshifts are due to the passage of  $Ly_{\alpha}$  from one filter to the other. As a general rule, the determination of the photometric redshifts should be rather accurate in the redshift range [3,5] even without the U or an infrared filter, but their presence is crucial for all other redshift ranges.

The quality of the  $z_{phot}$  determination is likely to improve if real quasar spectra are used. However, this implies that a spectral library is required, containing some hundreds of quasar spectra, with redshifts spanning from 0 to  $\sim 5$  and with a spectral coverage spanning from the ultra-violet to the infrared.

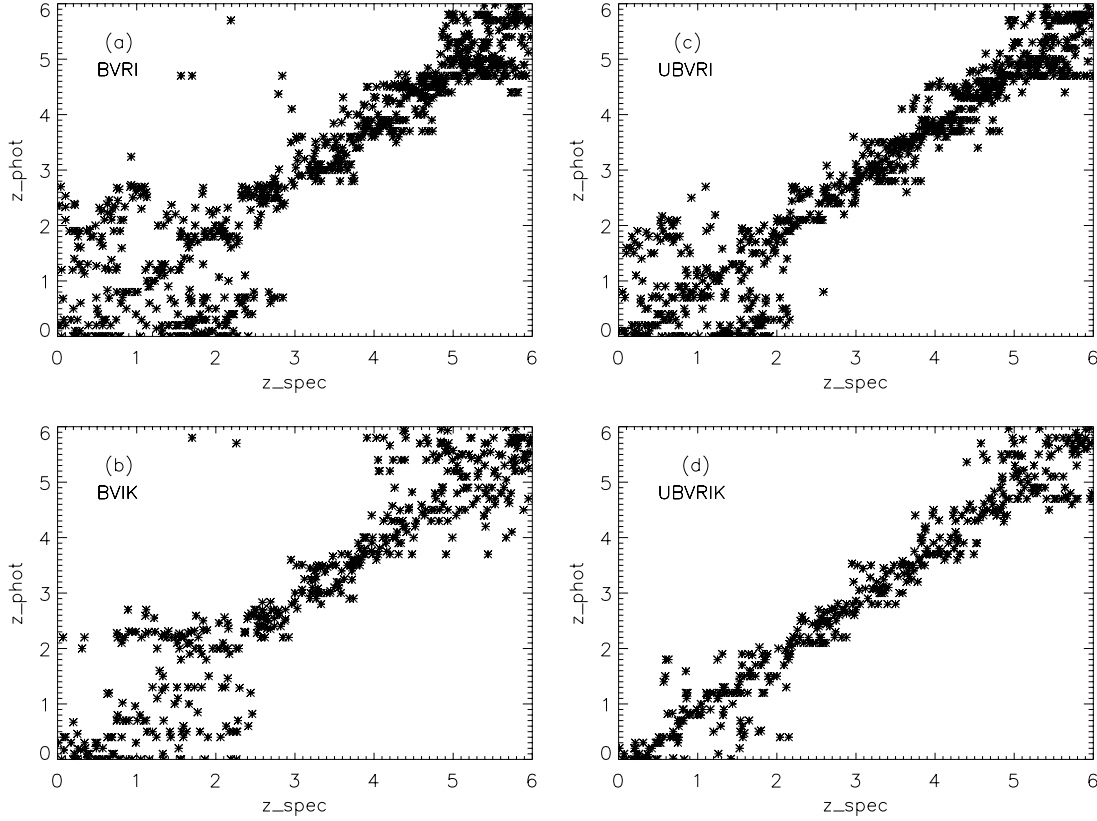


**Fig. 3a–d.** Photometric redshift versus model redshift for a simulated catalogue of 1540 quasars and 4 different filter combinations: BVRI **a**, BVIK **b**, UBVRI **c** and UBVRIK **d**.

#### 4.2. *C*, *CR* and *E* as a function of redshift

The *completeness*, the *confirmation rate* and, therefore, the *efficiency* of the method depend on the redshift. The demonstration of this dependence is easy to show for the *completeness*, but not for the *confirmation rate*. The *completeness* within redshift bins has the same definition as for the entire sample: the ratio between the number of real quasars with spectroscopic redshifts (hereafter  $z_{spec}$ ) within the examined bin, identified as candidates even if their  $z_{phot}$  is significantly different from their  $z_{spec}$ , over the estimated total number of quasars.

Fig. 4 illustrates the *completeness* versus the redshift, without  $\chi^2$  selection, for 4 different filter sets: the solid, dotted, dashed and dashed-dotted lines correspond to BVIK, UBVRH, UVK and BVRI, respectively. The *completeness* over the whole redshift range for this 4 filter combinations is in all cases more than 85%, as shown in Fig. 1a.

Fig. 4 reveals that, independently of the filter combination, the *completeness* is always lower in the redshift range [2,3] due, as already mentioned, to the stellar-like colors of quasars. This fact could certainly increase the number of quasar candidates within this range but it could also be a possible source of incompleteness, since some quasars will inevitably be classified as stars. Furthermore, different filter combinations offer a different *completeness* at different redshifts. The filter set BVIK assures a *completeness* of over 70% in the critical redshift range

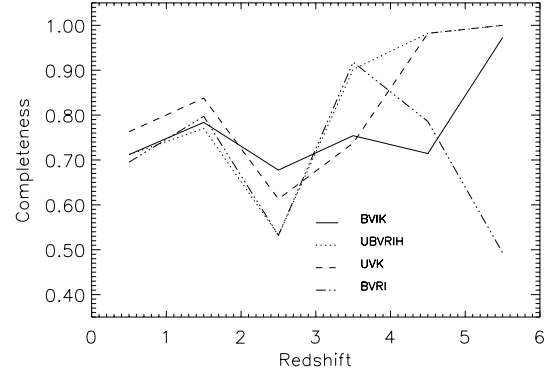


**Fig. 4.** Completeness versus redshifts for 4 different filter sets: — BVIK, ··· UBVRH, --- UVK, - · - · BVRI.

[2,3], which however remains low up to  $z \sim 5.5$ . UVK offers the possibility of a *completeness* of  $\sim 80\%$  for  $z < 2$ , while UBVRH results give a *completeness* over 90% for high- $z$  quasar samples ( $z > 3$ ).

Things become more complicated if one tries to make an equivalent evaluation of the *confirmation rate* within redshift bins. This time, the *confirmation rate* is the ratio between the number of real quasars with  $z_{phot}$  in the examined redshift bin, over the number of quasar candidates (quasars + possibly stars) with  $z_{phot}$  that belong to this particular redshift interval. Obviously, this definition depends on the accuracy of the determi-

nation of the  $z_{phot}$  as well as on the width of the redshift bins. Therefore, the dependence of the confirmation rate versus the redshift can be evaluated qualitatively but not quantitatively, and so it goes for the *efficiency* as well.

If the final aim of a survey is assembling a quasar sample with redshifts within a restrained interval, all candidates with a  $z_{phot}$  that lies outside this interval will, in principle, be rejected. In the more realistic case of an all redshift survey, the most interesting strategy is to simply optimize the spectroscopy towards the optical or the infrared wavelengths. The spectroscopy of quasars with redshifts up to  $\sim 3$  is much more interesting in the optical band, while higher redshift quasars should be spectroscopically observed in the infrared, since most of their emission lines are shifted to these wavelengths. The simulations have shown that, although the determination of quasar  $z_{phot}$  is sometimes dispersed at  $z \leq 2.5$  and  $z \geq 4.5$  (Fig. 3), this effect hardly translates into high- $z$  quasars ( $z > 4$ ) being wrongly identified as low- $z$  ones ( $z < 3$ ) or vice versa.

## 5. Applying the method to real samples

The method presented above has been tested on a series of samples found in the literature, giving rather satisfactory results. Depending on the sample and the available information, the *confirmation rate* and/or the *completeness* have been calculated.

### 5.1. The Deep Multicolor Survey

The Deep Multicolor Survey is an imaging survey covering 6 fields on a total area of 0.83 square degrees on the northern sky at high galactic latitude, carried out at the 4m Mayall telescope of the Kitt Peak National Observatory. 6 filters have been used, covering the wavelength range from 3000 to 10000 Å: U, B, V, R', I75 and I86, and a photometric catalogue of  $\sim 21000$  stellar-like objects has been assembled, with the aim of conducting a multicolor quasar search (Osmer et al. (1998) and the references therein). 137 stars, 49 compact narrow emission line galaxies (hereafter CNELGs), and 54 quasars with redshifts spanning from 0.3 to 4.3 have already been spectroscopically identified. These objects were the 240 quasar candidates selected by Hall et al. according to their position on color-color plots, a high fraction of them (194 objects) selected by the UVX technique (Hall et al., 1996). This selection favored quasars with redshifts less than 2.2. The redshift distribution of these objects can be seen in Fig. 5, where the spectroscopic sample is plotted by a dotted line.

For our purposes, we cut the catalogue at  $B=22.3$ , a limit at which the sample is almost 100% complete and only marginally contaminated ( $\sim 8\%$ ) by galaxies, and we only used objects for which photometry was available in all 6 filters. Hence, 3 of the spectroscopically confirmed quasars were excluded, and we ended up with a catalogue of 3720 stellar-like objects. For the magnitude limit and the area covered by the survey, approximately  $106_{-22}^{+27}$  quasars are expected to be found among the objects of the catalogue (HS90), resulting a *completeness* of at

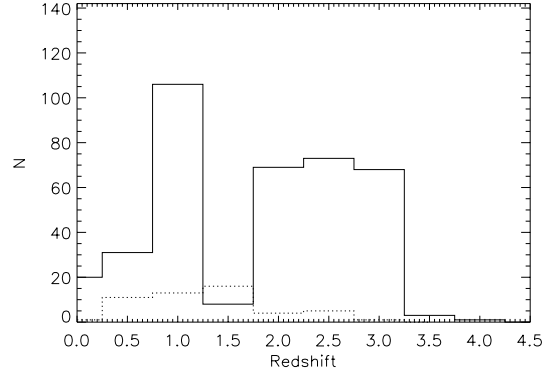


**Fig. 5.** Estimated redshift distribution of the photometrically selected candidates (solid line), spectroscopically determined sample of 51 DMS quasars (dotted line).

least 80% for the usual multicolor selection techniques (Hall, private communication) and  $\sim 88\%$  for our method.

Table 3 summarizes the characteristics of the different catalogues examined in this section: surface covered, magnitude limits, filters used, number of quasars, and number of candidates for different confidence levels. The expected number of stars on the DMS field has been computed from R95. In the case of the DMS field, the number of spectroscopically confirmed quasars is also given between brackets.

Among the 3720 objects in this catalogue, we identified 3332 as stars because their photometry shows a better match to the stellar templates. With our method, 6 of the 51 spectroscopically confirmed quasars (DMS0059-0056, DMS1358-0054, DMS1714+5012, DMS1714+5003, DMS1714-4959 and DMS1358-0055) are misclassified as stars. Only 7 of the 97  $B \leq 22.3$  candidates, spectroscopically identified as stars, but all 34  $B \leq 22.3$  CNELGs belong to our candidate list, if no  $\chi^2$  selection is made. At a 99% confidence level, 25 CNELGs are classified as quasar candidates.

To summarize, we find 388 quasar candidates for 106 actual quasars, with an expected *completeness* of  $45/51=0.88$  and an expected *confirmation rate* of  $(106 \times 0.88)/388=0.24$ , if no  $\chi^2$  selection is made. The equivalent values with 99% confidence level selection are 0.88 and 0.27, respectively, for 348 quasar candidates (see also Table 4).

Fig. 5 displays with a solid line the estimated redshift distribution of our 388 quasar candidates. The accumulation of identifications around  $z \sim 1$  is due to the CNELGs, with  $z_{spec}$  in the range  $[0.1, 0.8]$  typically, identified by our procedure as quasar candidates with  $z_{phot} \sim 1$ . The broad distribution at  $z \in [2.0, 3.0]$  is probably due to the stellar-like colors of quasars at these redshifts, which makes the distinction between stars and quasars particularly difficult by photometric means, increasing the number of quasar candidates, but it also corresponds to the expected maximum of the quasar space distribution. For comparison, we plot the redshift distribution of the 51 spectroscopically confirmed quasars (dotted line).

The above results are summarized in the first 6 columns of Table 4, where the values of the *completeness* (C), the *confir-*

**Table 3.** Quasars candidates for DMS, HDF<sub>Bright</sub> and Parkes selected by the  $z_{phot}$  method.

Survey	Surface covered	Mag. limit	Filters	Stars			Quasars			
				exp	cand	exp	95%	99%	no $\chi^2$	conf
DMS	0.83sd	B=22.3	U,B,V,R', I75,I86	3316 ± 60 (R95)	3332	106 <sup>+27</sup> <sub>-22</sub> (HS90)	295 (40)	348 (45)	388 (45)	51
HDF <sub>B</sub>	1.00sd	B=21.0	B,V,R	–	–	30	26	30	30	30
Parkes		H=19.6	B,V,R,I, J,H,K	–	–	129	99	107	125	129

**Table 4.** *Completeness* (C), *confirmation rate* (CR) and *efficiency* (E) for the samples DMS, HDF<sub>B</sub> and Parkes and for the simulated catalogues, with a  $\chi^2$  selection at 99% confidence level and without any  $\chi^2$  selection. In column 2 we give the same quantities for the DMS sample and for the usual multicolor selection techniques.

	DMS	$z_{phot}$		sim		HDF <sub>B</sub>		sim		Parkes		sim	
		99%	no $\chi^2$	99%	no $\chi^2$	99%	no $\chi^2$	99%	no $\chi^2$	99%	no $\chi^2$	99%	no $\chi^2$
C	0.80	0.88	0.88	0.79	0.86	1.00	1.00	0.74	0.76	0.83	0.97	0.52	0.81
CR	0.23	0.27	0.24	0.20	0.21								
E	0.18	0.24	0.21	0.16	0.18								

*mation rate* (CR) and the *efficiency* (E) are shown in columns 3 and 4. The values predicted by the simulations are also given for comparison in columns 5 and 6, using the same filter combinations as for the real data, and keeping the filter responses as close as possible to those actually used. Column 2 gives the same quantities for the DMS and the usual multicolor selection techniques. Note that the values given for the *completeness* and the *efficiency* are the lower estimations. The two methods give comparable values for all 3 quantities (C, CR and E), with a slightly better efficiency for the multicolor technique when a  $\chi^2$  criterion is imposed.

In order to estimate the contamination due to compact galaxies, we have added to the template library the spectra of blue starburst galaxies, obtained from the public model Starburst99 code by Leitherer et al. (1999), as well as a delta-burst model taken from the new Bruzual & Charlot evolutionary code (GISSEL98, Bruzual & Charlot 1993), and a set of 4 empirical SEDs compiled by Coleman, Wu and Weedman (1980) (hereafter CWW) to represent the local population of galaxies (E, Sbc, Scd and Im). Spectra from the Starburst99 code were selected with solar metallicity and Salpeter IMF, taking different ages for an instantaneous burst ranging from 1 to 20 Myr. In the case of the GISSEL98 delta-burst, the IMF is that of Miller & Scalo (1979), with solar metallicity and 51 different ages ranging from 0.001 to 20 Gyr. CWW spectra were extended to wavelengths  $\lambda \leq 1400 \text{ \AA}$  and  $\lambda \geq 10000 \text{ \AA}$  using the equivalent GISSEL98 spectra.

When applying the method to the DMS sample of 3523 stellar objects (we remind here that we only use objects with photometry in all 6 filters), using the template library extended with galaxy spectra, we find that  $\sim 80\%$  of them are better fitted by stellar or quasar templates rather than by galaxy spectra. This fraction is only 56% for the subsample of 97 objects spectroscopically identified as stars. Among the subsample of the 51

objects spectroscopically identified as quasars, there are 38% that show a better fit to the galaxy spectra, and 80% among them correspond in particular to genuine young starbursts according to the best-fit spectra, with ages ranging between 1 and 20 Myrs. The result is different when the same extended template library is applied to the 34  $B \leq 22.3$  DMS CNELGs. In this case, 85% of the sample (29 objects) is well fitted by galaxy spectra rather than quasar or stellar templates. The fraction of best-fit galaxy templates corresponding to young starbursts is  $\sim 2/3$ . Generally speaking, a typical fraction between 1/4 and 1/3 of the quasar candidates is also compatible with young starbursts, and CNELGs are hardly selected as quasars, when supplementary galaxy templates are used.

To summarize, adding star-bursting and early-type galaxy templates does not give a better solution to the problem of selecting quasar candidates: if star-burst candidates are included in the list, the number of candidates is multiplied by a factor of 4 to 5. On the other side, objects like CNELGs will not be mixed with the quasar candidates but we take the risk to miss  $\sim 35\%$  of the quasars, identified as star-bursting galaxies. However, for the purposes of a survey, all objects will be tested through the same, general pipeline. Some objects (like quasars and compact blue galaxies) will inevitably end up as candidates in more than one list, depending on the different selection criteria.

### 5.1.1. Quasar photometric redshifts

Fig. 6 left presents the  $z_{phot}$  versus  $z_{spec}$  for the 51 DMS quasars. For 23 of them,  $|z_{phot} - z_{spec}| \leq 0.1$ . We note an important dispersion for redshifts lower than typically 2.5: quasars with a  $z_{spec} \in [1, 2]$  are better fitted by templates of quasars with  $z \in [0, 1]$ . This is also the tendency arising from simulations and shown on Fig. 3 (upper right), for the filter combination UBVRI.

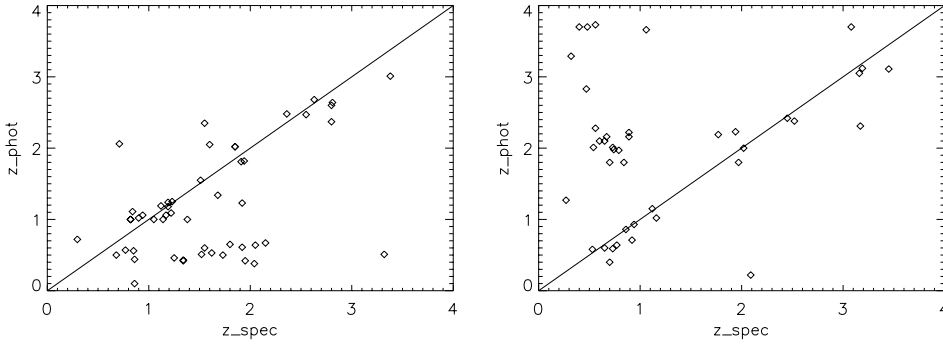


**Fig. 6.** Photometric redshifts versus spectroscopic redshifts for the 51 quasars of the DMS sample (left) and for the new sample of 46 spectroscopically confirmed quasars (Hall, private communication) (right).

Fig. 6 right presents the  $z_{phot}$  versus  $z_{spec}$  for a new sample of 46 spectroscopically identified quasars (Hall et al., 2000). 17 of them have  $|z_{phot} - z_{spec}| \leq 0.1$ . This time we note that quasars with a  $z_{spec} \in [0, 1]$  are better fitted by quasars with  $z \in [1, 2]$ , and this trend is also seen on the simulations (Fig. 3 upper right) for the same set of filters.

### 5.2. $HDF_{Bright}$ and Parkes

The *completeness* has also been tested on two recently published quasar catalogues. Liu et al. (1999) published a list of 30 spectroscopically confirmed quasars with their photometry in B, V and R. These objects have  $17.6 \leq B \leq 21.0$  and  $0.44 \leq z \leq 2.98$ , and were selected on a one square degree field centered on the HDF North. They were firstly identified as quasar candidates by their (B-V) (V-R) colors, along with 31 other candidates that, after the spectroscopy, turned out to be stars.

With our method we identified all 30 quasars as quasar candidates. However, the limited number of filters did not allow us to reduce the number of stars selected as quasar candidates, 30 out of 31 were in our own list.

We also applied our method to the Parkes subsample published by Francis et al. (1999). Only point-like objects, with the photometry in all 7 filters (B, V, R, I, J, H,  $K_n$ ) were kept, thus 129 out of the 157 quasars of the initial sample remain in our catalogue. At a confidence level of 99%, 107 among these objects were classified as quasar candidates (*completeness*=0.83). If no  $\chi^2$  selection is applied, the *completeness* is equal to 0.97.

Columns 7 to 14 in Table 4 summarize these results. Simulation results are also given for comparison. Note that in both cases, the *completeness* for the real samples is found to be even higher than expected according to the simulations.

*Confirmation rate* and *efficiency* cannot be computed for these two samples, since the entire point-like object catalogues (including stars) are not available.

### 5.3. EIS-wide (patch B)

An attempt to apply our method to the EIS-wide (patch B) data was made. The results are approximatively the same as those obtained in multicolor procedures. This was somewhat expected: the multicolor approach proposed here, when applied to a 3 filter data set, is equivalent to a color-selection technique. Note that 3 filters have been used to carry out this survey: B, V

and I. On a (B-V) (V-I) diagram, quasar evolutionary tracks up to a redshift of  $\sim 3.3$  and the Main Sequence stars mix together.

## 6. Discussion

The quasar multicolor selection technique presented in this paper has some advantages as compared to the “traditional” color-color methods. First, it has the advantage of selecting quasar candidates even at redshifts where quasar and stellar colors are very much alike (2.5–3.0). However, the *efficiency* varies with the redshift. Independently of the filter set, some quasars with redshifts lying in the interval [2.5,3] will be skipped. Furthermore, the number of quasar candidates with estimated  $z_{phot}$  within this range will be far higher in comparison to other redshift bins. The set of filters used plays an important role in these results. Adding a filter is not necessarily equivalent to adding information and does not always improve the results, but imposes more stringent constraints by increasing the number of degrees of freedom. For this reason, a  $\chi^2$  selection does not improve the results in all cases.

This technique gives also an estimate of the (photometric) redshift of the candidates, and it is thus able to improve the spectroscopic follow up of a given sample. In some cases, which depend (again) on the filter combination and the redshift of the objects, this determination can be accurate ( $|z_{phot} - z_{spec}| \leq 0.1$ ). In most cases, quasars at redshift  $z \leq 3$  will not be misidentified at  $z \geq 4$  and vice versa, therefore the spectroscopy can be reliably targeted towards the optical or the infrared bands.

For the purposes of a survey aiming in assembling a quasar catalogue with a minimum cost, adding star-bursting and early-type galaxy templates does not appear as a priority. On the contrary, this addition will cause either the increase of the candidates by a factor of almost 5 (if star-burst candidates are considered as possible quasars) or the decrease of the *completeness*  $\sim 40\%$  (because an important fraction of real quasars will be better fitted by star-burst galaxies templates). For practical purposes (e.g the VIRMOS survey), when all the sources examined through the same pipeline, a fraction of objects identified as quasars will be also found within the “starburst” sample, but this does not affect the present selection.

The same method can be extended towards different directions. First, it can be adapted to particular objects like very red quasars, by adding the suited templates. However, this has to be done thoroughly, to prevent from a possible and undesirable in-

crease of the quasar candidates. It can also be used on spatially resolved objects, like Seyfert galaxies, because by construction, the software is independent of the morphology of the objects. This can be done by adding a stellar component to the AGN simulated spectra already used. Last but not least, it can be extended to very high redshifts (higher than 6), after an appropriate modeling of the intergalactic absorption.

As already mentioned, this software has been developed for the needs of preparing the quasars/AGN sample assembled in the future VIRMOS survey. However, the results and conclusions of this paper apply to all multicolor surveys in general. A cross-identification between optical and X-ray sources can be extremely useful, when X-ray data are available, and can increase the *efficiency*, as quasar candidates with a compact X-ray counterpart will have an even higher chance of being real quasars.

*Acknowledgements.* We would like to thank M. Bolzonella, J. P. Picat and M. Elvis for useful discussions. We would also like to thank the referee, Dr. P. Hall for his very useful comments that led to the improvement of our work.

## References

- Bolzonella M., Miralles J.M., Pelló R., 2000, submitted to A&A, preprint astro-ph/0003380
- Boyle B.J., Jones L.R., Shanks T., 1991, MNRAS 251, 482
- Bruzual G., Charlot S., 1993, ApJ 405, 538
- CUQS: <http://sa1.star.uclan.ac.uk/prn/cuqs.html>
- Cohen J., Hogg D., Blandford R., et al., 1999, accepted for publication in ApJ, astro-ph/9912048
- Coleman D.G., Wu C.C., Weedman D.W., 1980, ApJS 43, 393
- Fan X., 1999, AJ, 117, 2528
- Francis P.J., Whiting M.T., Webster R.L., 2000, PASA 17, 56
- Glazebrook K., Ellis R., Colless M., et al., 1995, MNRAS 273, 157
- Hall P.B., Osmer P.S., Green R.F., Porter A.C., Warren S.J., 1996a, ApJSS 104, 185
- Hall P.B., Osmer P.S., Green R.F., Porter A.C., Warren S.J., 1996b, ApJ, 462, 614
- Hartwick F., Schade D., 1990, ARA&A 28, 437
- Jarvis R.M., MacAlpine G.M., 1998, AJ 116, 2624
- Kennefick J.D., Osmer P.S., Hall P.B., Green R.F., 1997, AJ 114, 2269
- Krisciunas K., Margon B., Szkody P., 1998, PASP 110, 1342
- Leitherer C., Schaerer D., Goldader J.D., et al., 1999, ApJS 123, 3
- Liu M.C., Dey A., Graham J.R., et al., 2000, to appear in the June issue of AJ
- Madau P., 1995, ApJ 441, 18
- Miller G.E., Scalo J.M., 1979, ApJS 41, 513
- Miller L., Mitchell P.S., 1988, in: Osmer P, Phillips M.M. (eds.), Proceedings of a Workshop on Optical Surveys for Quasars, ASP Conference Series, Vol. 2, San Francisco: ASP, p. 114
- Miralles J.M., Pelló R., 1998, astro-ph/9801062
- Newberg H.J., Yanny B., 1997, ApJSS 113, 89
- Osmer P., Kenefick J.D., Hall P.B., Green R.F., 1998, ApJS 119, 189 <http://www.astronomy.ohio-state.edu/posmer/DMS/>
- Pelló R., Kneib J.-P., Bolzonella M., Miralles J.-M., 1999, Proceedings of the “Photometric Redshifts and High Redshift Galaxies”, Pasadena, PASP Conf. Ser. 191, p. 247. [astro-ph: 9907054]
- Peri F., Iovino A., Hickson P., 1997, “Quasar Detection using Multi-Narrow-Band Photometry”, in: *Science with Liquid Mirrors Telescopes*, Proceedings of the Marseille Meeting on LMTs, April 1997, in press.
- Peterson B.M., 1997, in: An introduction to active galactic nuclei, Cambridge University Press
- Pickles A.J., 1998, PASP 110, 863
- Prandoni I., Wichmann R., da Costa L., et al., 1999, A&A 345, 448
- Robin A., Haywood M., Gazelle F., et al., 1995, “Model of Stellar Population Synthesis of the Galaxy”, [http://WWW.obs-besancon.fr/www/modele/modele\\_ang.html](http://WWW.obs-besancon.fr/www/modele/modele_ang.html)
- Schade D., Lilly S.J., Crampton D., et al., 1995, ApJL 451, 1
- Wang T.G., Lu, Y.J., Zhou Y.Y., 1998, ApJ 493, 1
- Wolf C., Meisenheimer K., Roeser H.-J., et al., 1999, A&A 343, 399